Gluing Bifurcation and Noise-Induced Hopping in the Oscillatory Phenomena of Compartmentalized Bidisperse Granular Gases

Yinchang Li (李寅闿), Rui Liu (刘锐),* and Meiying Hou (厚美瑛)

*Beijing National Laboratory for Condensed Matter Physics and CAS Key Laboratory of Soft Matter Physics,
Institute of Physics, Chinese Academy of Sciences, Beijing 100190, China*
(Received 16 May 2012; published 5 November 2012)

Oscillatory phenomena of compartmentalized bidisperse granular gases are studied through experiments, molecular dynamics simulations, and a flux model [Mikkelsen *et al.*, Phys. Rev. E **70**, 061307 (2004)]. The degenerate oscillatory state (d-OSC), which has been predicted in our previous simulations [Liu *et al.*, Phys. Rev. E **79**, 052301 (2009)], is experimentally observed and well described by the flux model. From the d-OSC state, the system takes a transition to a complete oscillatory state (OSC) through a homoclinic gluing bifurcation. Around the bifurcation point, noise-induced periodic irregularity is observed, and it can be perfectly reproduced by simulations and the flux model with additional random flux terms. The numerical results show a low-frequency divergence characteristic of the irregular oscillation, which is clearly caused by noise-induced hopping between OSC and d-OSC states.

In some dynamical systems, two or more attractors may simultaneously coexist and can be merged through a gluing bifurcation. The dynamics of such systems may be dominated by noise. In particular, hopping can occur between attractors when the noise amplitude is comparable to the distance between attractors. Gluing bifurcations have been observed with interesting dynamical behaviors in many physical systems, such as electronic circuits [1], nonlinear optics [2], and fluid or liquid-crystal flows [3–7], etc., while hopping effects between attractors have been found in systems with large fluctuations, which induce $1/f$-type low-frequency divergent stochastic behaviors [8,9].

Recently, granular gases in compartmentalized systems have been found to exhibit rich nonequilibrium dynamical behaviors, including granular Maxwell's demon [10–13] and its extensions [14–19] in monodisperse systems, competitive asymmetric clustering (ASC) [20,21] and oscillations (OSC) [22–26] in bidisperse systems, etc. In one of our latest papers [27], we predicted a degenerate oscillation (d-OSC) in the compartmentalized bidisperse granular gas. In a d-OSC state, the oscillatory behavior of the larger particles in the gas is suppressed due to dissipation, and the phase trajectory of the whole system consists of two symmetry-degenerate limit cycles. There is a transition from a d-OSC to an OSC state, and we propose that it is triggered by a homoclinic gluing bifurcation. During the gluing process, apparent hopping effect is expected, due to the extreme intrinsic noise of the dilute granular system.

In this Letter, we show the first experimental observation of the d-OSC state and the gluing bifurcation in compartmentalized bidisperse granular gases. Based on Mikkelsen *et al.*'s flux model (FM) [20,21], a theoretical description for the related dynamical behaviors is given. A complete phase diagram is mapped out from experimental data and theoretical calculations, which complements our previous

simulation results [27]. The gluing process is further studied through numerical simulation and theoretical modeling. For the first time, the effects of noise are considered for the bidisperse system, and a hopping phenomenon is observed in either an OSC or a d-OSC state near the gluing point, which is seldom reported in two-dimensional systems.

In our experiments, a setup with two compartments connected by a rectangular window in the middle wall is used. The two compartments are identical, each with a ground area $\Omega = 26 \times 26$ mm². The connecting window, with width $W = 20$ mm and height $H = 30$ mm, is horizontally centered, and its lower edge is $h = 15$ mm above the bottom plate of the container. The whole container is fixed on an electromechanical shaker which moves in a sinusoidal manner with shaking frequency $f = 60$ Hz and adjustable amplitude A. Two kinds of particles, glass beads with radius $r_1 = 0.5$ mm and steel beads with $r_2 = 0.75$ mm (subscript 1 for glass and 2 for steel here and below) are used to compose a bidisperse granular gas. The mass ratio of the two species, m_1/m_2, is about $1/9$. The population of species i in the compartment α is denoted as $N_{i\alpha}$ [$i = 1, 2$ for the two species; $\alpha = l, r$ for the left compartment (LC) or the right one (RC)]. The total number of beads is fixed to be $N = 1000$, and the number fraction $\Phi_i = N_i/N$ is varied, where N_i is the number of beads for species i. The intensity of the vibration is characterized by the dimensionless peak velocity of the vibrating plate $v_b = 2\pi A f/\sqrt{4gr_1}$.

As we have predicted in previous simulations [27], five basic states of the system are experimentally observed with different v_b and Φ_2, including the trivial homogeneous state (HOM) at large v_b, the ASC state at small v_b, the OSC and d-OSC states at relatively small Φ_2 ($\Phi_2 < 0.5$ in this system) and intermediate v_b, and the s-HOM state
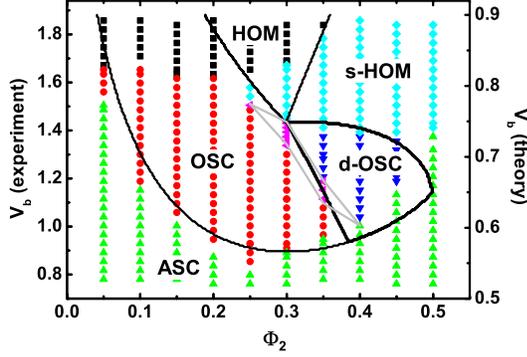
FIG. 1 (color online). Phase diagram in the Φ_2-v_b plane: symbols for experimental results and plates separated by solid lines for calculations through FM without noise terms. Irregular oscillations are experimentally observed in the gray polygon.

[smaller (lighter) glass beads are nearly homogeneously distributed, and larger (heavier) steel beads are asymmetrically clustered], which is a concomitant clustering state of the d-OSC state and cannot be distinguished from the ASC state at large Φ_2. The corresponding phase diagram is shown with symbols in Fig. 1. To focus on the structure around the oscillatory regimes, data for very large v_b and Φ_2 are not plotted.

Snapshots of an OSC state at $v_b = 1.04$ and a d-OSC state at $v_b = 1.23$ for $\Phi_2 = 0.35$ are shown in Fig. 2. In the conventional single-limit-cycle OSC state [Figs. 2(a)–2(d)], two kinds of particles fully participate the oscillation, and they both get clustered alternatively in the two compartments. In the d-OSC state [Figs. 2(e)–2(h)], most steel beads always stay in one compartment; only a very small
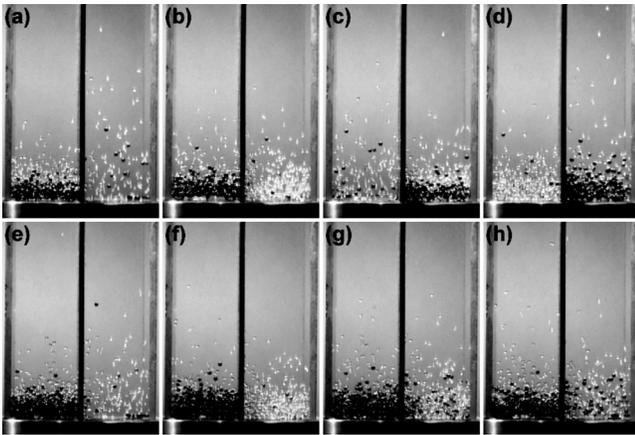

FIG. 2. Experimental snapshots for $\Phi_2 = 0.35$, the OSC state observed at $v_b = 1.04$ [(a–d)], and the d-OSC state at $v_b = 1.23$ [(e–h)]: (a) and (e) Both species are mostly clustered in LC; (b) and (f) glass beads are driven to RC; (c) and (g) steel beads start to follow the glass beads to move to RC; (d) and (h) most glass beads return to LC; the next state would be similar to (a) and (e) if steel beads return to LC. Glass beads are in light color, and steel ones in dark.

number of them can be exchanged between the two compartments and oscillate with most glass beads. Thus symmetric double-limit cycles are observed for the d-OSC state in the phase plane spanned by $N_{1\alpha}$ and $N_{2\alpha}$.

We have demonstrated that the OSC state can be well described by FM in a previous study [27]. The d-OSC state can also be understood by the same model. By adopting all the assumptions and deductions in Refs. [20,21], a flux function, which measures the outflow flux of species i from one compartment α to the other, is given as

$$F_i(N_{1\alpha}, N_{2\alpha}) \propto N_{i\alpha} \nu_{i\alpha} e^{-gh/\nu_{i\alpha}^2}(1 - e^{-gH/\nu_{i\alpha}^2}), \quad (1)$$

where $\nu_{i\alpha} = \sqrt{T_\alpha/m_i}$ with Boltzmann's constant $k_B = 1$. The common granular temperature T_α for both species in compartment α is determined by the energy balance between dissipation and injection. The dissipation caused by particle-particle collisions is in the form of $Q_{pp}^\alpha \propto T_\alpha^{1/2}$. Assuming a sawtooth motion of the bottom, the energy input rate J does not depend on the granular temperature T_α explicitly. Mikkelsen *et al.* did not consider the dissipation of particle-wall (pw) collisions; however, we could obtain a better agreement (which will be explained later) with our experiments if it is considered. For simplicity, we suppose that both species have the same coefficient of restitution ϵ in either a particle-particle collision or a pw collision. Following Mikkelsen *et al.*'s formulation, it is easy to show that the dissipation of the pw collision involving the surrounding walls is $Q_{pw}^\alpha \propto T_\alpha^{3/2}$, and that with the bottom plate will result in a negative term proportional to $T_\alpha^{1/2}$ in J, which decreases the energy input efficiency [28]. Thus, a cubic equation in the form of $AT_\alpha^{3/2} + BT_\alpha^{1/2} + C = 0$, where A, B, and C are functions of $N_{i\alpha}$ and m_α, is finally obtained for $T_\alpha^{1/2}$ with the assumption of a balance between dissipation and injection. An analytical solution for this equation exists, and the flux function in Eq. (1) can be calculated.

The dynamical behaviors of the whole system could be simply described by the following equations:

$$\frac{dN_{il}}{dt} = -\frac{dN_{ir}}{dt} = -F_i(N_{1l}, N_{2l}) + F_i(N_{1r}, N_{2r}). \quad (2)$$

By using the explicit fourth-order Runge-Kutta method, these equations are numerically solved, and all five states are obtained, with the phase diagram shown by solid lines in Fig. 1. Compared with the experimental results, the theory describes the system well with the above settings, ignoring some mismatch in v_b. If the dissipation in pw collisions is not considered, the domains of OSC and d-OSC states will be rather narrow, though no qualitative change will be introduced in the phase diagram.

In Fig. 3, we show the phase orbits of OSC and d-OSC states obtained by numerical solution of the model, single-limit cycle, and symmetric double cycles are obtained, respectively. The transition from d-OSC to OSC
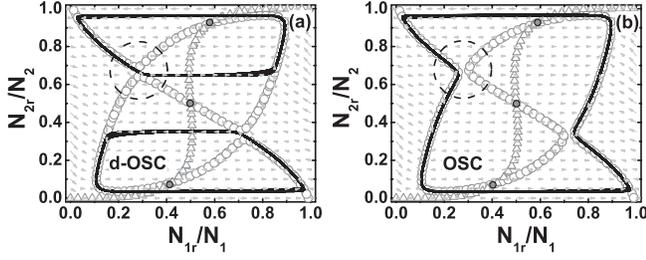
FIG. 3. For $\Phi_2 = 0.35$, phase trajectories of the d-OSC state with symmetric double cycles at $v_b = 0.651$ (a) and OSC state with a single cycle $v_b = 0.649$ (b) near the gluing point are plotted by solid curves, hollow symbols (circles for dN_{1r}/dt, triangles for dN_{2r}/dt) show the nullclines of the net flux of both species, and arrows represent the whole flow diagram.
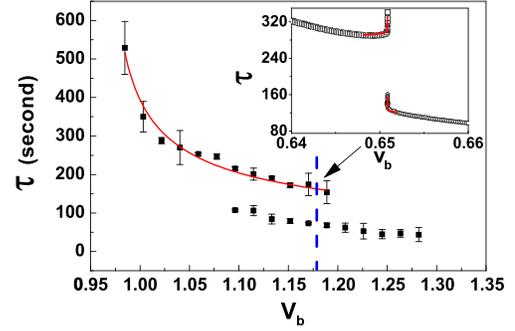

FIG. 4 (color online). Recurrence time for the oscillatory states obtained in experiments. The inset shows the theoretical prediction near the gluing point (v_b matched according to Fig. 1).

(decreasing v_b) is through a homoclinic gluing bifurcation, in which the double cycles are opened by the unstable domain of the saddle center and get joined in the periphery. The nullcline of the net flux ($dN_{i\alpha}/dt$) of glass beads takes some topology-invariant rearrangement at the contact point (as shown in the dashed circle), while that of the steel beads does not change much. One saddle center and two unstable foci exist (gray dots in the figure) in this d-OSC and OSC states, which differs from the OSC cycle with only one unstable focus that we have previously studied [27]. By decreasing v_b to values far away from the gluing point, the three unstable fixed points here will be merged into one unstable focus via a symmetric saddle-node (unstable) like bifurcation, and the previously reported OSC state can be reached.

An irregular oscillation (i-OSC), which behaves like a random mixture of d-OSC and OSC states, is also observed around the boundary of the two states (gray polygon shown in the phase diagram in Fig. 1), and this phenomenon cannot be explained by the current theory. The period (or recurrence time) τ of the oscillatory states is measured in our experiments by observing the recurrence of density patterns in the two compartments with the aid of high speed imaging and autodetection programs. As shown in Fig. 4, when v_b is either small or large, i.e., the system is in a pure state of either OSC or d-OSC, the recurrence time is well single-valued. The period τ of a pure OSC state at small v_b obeys $\tau \sim (v_b - v_{ic})^{-1/2}$ (red line in the figure), corresponding to an infinite-period bifurcation from OSC to ASC with critical shaking velocity v_{ic}, while τ of a pure d-OSC state at large v_b is about $O(1)$, corresponding to a supercritical Hopf bifurcation from s-HOM to d-OSC. In the intermediate regime ($1.08 < v_b < 1.20$), the recurrence time is somewhat irregular, and the recurrent phenomena are found to be sometimes in an OSC orbit and sometimes in a d-OSC one. The recurrence time data measured are classified according to the two behaviors, and two statistical values are finally obtained and shown in the figure. This hopping behavior can happen only near the gluing point when the two limit cycles of the d-OSC state

are close enough or two points in the single-limit cycle of OSC are near enough so that noise can activate hopping. Thus it is a sign of the gluing process from a d-OSC to OSC state. However, in the above theory without any consideration of noise, a divergence in the recurrence time, instead of irregularity, is obtained (as shown in the inset, where the red lines are logarithmic fits to show the divergence), which is typical for a homoclinic bifurcation.
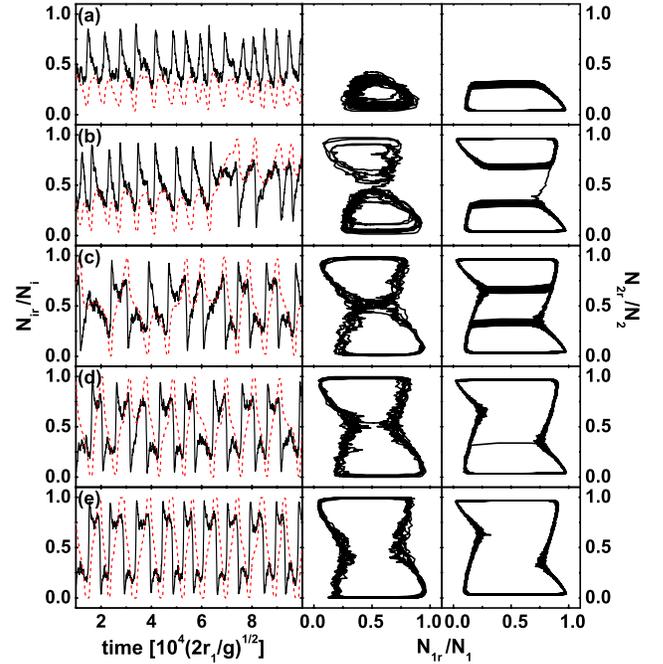

FIG. 5 (color online). Time evolution of populations for the right compartment (left panel: black solid lines for N_{1r}/N_1 and red dashed lines for N_{2r}/N_2) and phase trajectories (middle panel) given by MD simulation at $\Phi_2 = 0.275$, and $v_b = 0.545$ (a), 0.535 (b), 0.525 (c), 0.520 (d), and 0.510 (e). The theoretical correspondences obtained from Eq. (2) with noise terms in Eq. (3) are shown in the right panel, with the confining parameters $K_1^2 = 3$ and $K_2^2 = 1$.
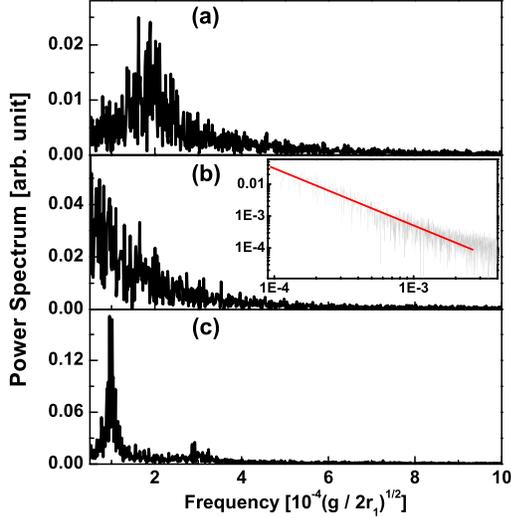
FIG. 6 (color online).   Fourier transformation of the time series obtained through simulation in Fig. 5: $v_b = 0.545$ (a), 0.525 (b), and 0.510 (c). The inset in (b) is a log-scale plot of the data, which shows a $1/f$ frequency divergence.

It is beyond our devices' ability to do detailed measurements around the gluing point. We implement the molecular dynamics simulation (MD) to study the gluing process. A standard hard-sphere event-driven algorithm [29,30] is used to simulate a system with the same geometric parameters as those in the experiments. Meanwhile, noisy flux terms $\xi_{i\alpha}$ are introduced into the right-hand side of Eq. (2), by simply assuming that the flux fluctuation of either species is independent from the other. Thus the Gaussian fluctuation form suggested by Eggers [11] for monodisperse systems can be used, with the correlation functions as follows:

$$\langle \xi_{i\alpha}(t)\xi_{j\beta}(t')\rangle = \sigma^2(N_{i\alpha})\delta_{ij}\delta_{\alpha\beta}\delta(t-t'), \qquad (3)$$

where $\sigma^2(N_{i\alpha}) = K_i^2[F(N_{i\alpha}) + F(N_i - N_{i\alpha})]$ and K_i^2 is a system parameter that confines the noise amplitude [31]. The values of K_i^2 only determine how close to the gluing point that one can observe the hopping effect. In our simulations, $K_1^2 \sim 3$ and $K_2^2 \sim 1$ are measured near the gluing point.

The results from MD simulation and FM theory in Fig. 5 show clearly how the noise affects the gluing process. When v_b is properly large, the system, represented by $\{N_{1\alpha}, N_{2\alpha}\}$, stays in one of the symmetric double-limit cycles of the d-OSC state. As v_b decreases and approaches the critical value, the system can jump over to the other limit cycle, and two sequential jumps will lead to an OSC-like behavior. In the immediate vicinity of the gluing point, it is impossible to distinguish d-OSC and OSC states from each other. By further decreasing v_b, the system becomes mainly OSC-like, but two sequential jumps between the *nearest* points may result in a d-OSC like behavior. Finally, only the OSC state is possible when v_b is small enough.

The FM theory with flux fluctuation exhibits qualitatively the same behaviors, which are shown in the right panel of Fig. 5.

The data sequences for both d-OSC and OSC states show strong periodicity, with sharp peaks in their power spectrums, as shown in Fig. 6. However, the power spectrum for the transient i-OSC state almost exhibits no obvious periodicity; instead, a $1/f$-type low-frequency divergence is observed, which is characteristic of such hopping phenomena.

In conclusion, we have observed a homoclinic gluing bifurcation in a granular system for the first time, which enriches the nonequilibrium dynamics of the system and may make it to be a model system for nonlinear dynamics. We have also found that noise plays an important role in the system, which induces a striking hopping effect and leads to a low-frequency divergent i-OSC state around the gluing point. We will check the possibility to chaos if the system is extended to higher dimensions with more species or more compartments in further studies.

*lr@iphy.ac.cn

[1] P. Glendinning, J. Abshagen, and T. Mullin, Phys. Rev. E **64**, 036208 (2001).
[2] R. Herrero, J. Farjas, R. Pons, F. Pi, and G. Orriols, Phys. Rev. E **57**, 5366 (1998).
[3] E. Meron and I. Procaccia, Phys. Rev. A **35**, 4008 (1987).
[4] J. Abshagen, G. Pfister, and T. Mullin, Phys. Rev. Lett. **87**, 224501 (2001).
[5] G. Demeter and L. Kramer, Phys. Rev. Lett. **83**, 4744 (1999).
[6] G. Demeter, D. O. Krimer, and L. Kramer, Phys. Rev. E **72**, 051712 (2005).
[7] V. Carbone, G. Cipparrone, and G. Russo, Phys. Rev. E **63**, 051701 (2001).
[8] F. T. Arecchi and F. Lisi, Phys. Rev. Lett. **49**, 94 (1982).
[9] F. T. Arecchi, R. Meucci, G. Puccioni, and J. Tredicce, Phys. Rev. Lett. **49**, 1217 (1982).
[10] H. J. Schlichting and V. Nordmeier, Math. Naturwiss. Unterr. **49**, S323 (1996).
[11] J. Eggers, Phys. Rev. Lett. **83**, 5322 (1999).
[12] J. J. Brey, F. Moreno, R. García-Rojo, and M. J. Ruiz-Montero, Phys. Rev. E **65**, 011305 (2001).
[13] A. Lipowski and M. Droz, Phys. Rev. E **65**, 031307 (2002).
[14] K. van der Weele, D. van der Meer, M. Versluis, and D. Lohse, Europhys. Lett. **53**, 328 (2001).
[15] D. van der Meer, K. van der Weele, and D. Lohse, Phys. Rev. E **63**, 061304 (2001).

[16] D. van der Meer, K. van der Weele, and D. Lohse, Phys. Rev. Lett. **88**, 174302 (2002).

[17] F. Coppex, M. Droz, and A. Lipowski, Phys. Rev. E **66**, 011305 (2002).

[18] F. Cecconi, A. Puglisi, U. M. B. Marconi, and A. Vulpiani, Phys. Rev. Lett. **90**, 064301 (2003).

[19] U. M. B. Marconi and M. Conti, Phys. Rev. E **69**, 011302 (2004).

[20] R. Mikkelsen, D. van der Meer, K. van der Weele, and D. Lohse, Phys. Rev. Lett. **89**, 214301 (2002).

[21] R. Mikkelsen, D. van der Meer, K. van der Weele, and D. Lohse, Phys. Rev. E **70**, 061307 (2004).

[22] R. Lambiotte, J. M. Salazar, and L. Brenig, Phys. Lett. A **343**, 224 (2005).

[23] G. Costantinia, D. Paolotti, C. Cattuto, and U. M. Bettolo Marconi, Physica (Amsterdam) **347A**, 411 (2005).

[24] T. Miao, Y. Liu, F. Miao, and Q. Mu, Chin. Sci. Bull. **50**, 726 (2005).

[25] S. Viridi, M. Schmick, and M. Markus, Phys. Rev. E **74**, 041301 (2006).

[26] M. Hou, H. Tu, R. Liu, Y. Li, K. Lu, P. Y. Lai, and C. K. Chan, Phys. Rev. Lett. **100**, 068001 (2008).

[27] R. Liu, Y. Li, and M. Hou, Phys. Rev. E **79**, 052301 (2009).

[28] Y. Li, R. Liu, M. Shinde, and M. Hou, Granular Matter **14**, 137 (2012).

[29] D. C. Rapaport, *The Art of Molecular Dynamics Simulation* (Cambridge University Press, Cambridge, England, 1997).

[30] T. Pöschel and T. Schwager, *Computational Granular Dynamics: Models and Algorithms* (Springer, Berlin, 2005).

[31] R. Mikkelsen, K. van der Weele, D. van der Meer, M. van Hecke, and D. Lohse, Phys. Rev. E **71**, 041302 (2005).